Bragging About Diffraction

Harel Yona, Rachel Finkelshtein

Contents

I Introduction

X-ray diffraction is a technique for investigating the atomic structure of crystalline materials. When X-rays interact with the periodic arrangement of atoms in a crystal, they are scattered. Under certain conditions, this scattering leads to constructive interference, which amplifies the resulting diffracted wave. This phenomenon is described quantitatively by **Bragg's Law**,

$$n\lambda = 2d\sin\theta \tag{1}$$

which relates the wavelength of the incident wave (λ), the spacing between atomic planes (d), and the angle of incidence (θ) at which constructive interference occurs. The variable n is an integer representing the order of diffraction.

In natural crystals, the atomic planes are spaced on the order of angstroms, and therefore X-rays, which have comparably short wavelengths, are required to probe their structure. However, Bragg's Law is not limited to atomic systems. Any periodic structure with spacing comparable to the wavelength of the probing radiation will exhibit similar diffraction behavior. In our experiment, we scaled up the system: instead of atoms, we used a Styrofoam cube containing a regular array of metal spheres to represent a simplified lattice. We then used microwaves—whose wavelength is roughly 50,000 times longer than that of X-rays—to observe analogous diffraction effects. This approach allows us to visualize the same principles that govern X-ray crystallography, using macroscopic components.

Before investigating diffraction, we verified that the transmitter and receiver act as polarizers by measuring the angular dependence of transmitted intensity. The results followed Malus' Law,

$$I = I_0\cos^2\theta \tag{2}$$

confirming polarization behavior. The calculation and corresponding figure are provided in Appendix A.

A Planes of Incidence

In this experiment, Bragg diffraction is analyzed with respect to two distinct planes, illustrated in Figure 1 (depicted in red and green). Each plane defines a different angle of incidence, denoted θ and θ', respectively. By basic geometric considerations, the relationship between the angles is given by $\theta' = \theta + 45°$. An additional characteristic of the diagonal incidence plane is the increased spacing between scattering centers (metal balls), which is $\sqrt{2}d$.

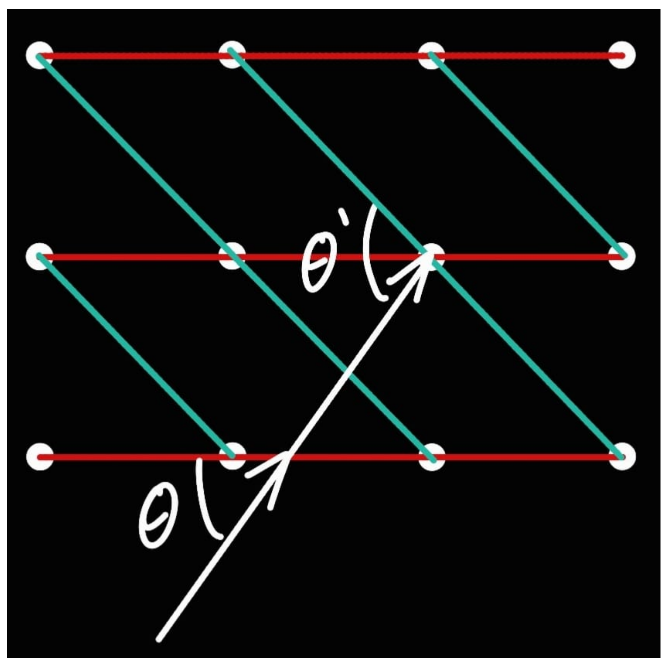

Figure 1: Schematic illustration of Bragg diffraction occurring along two planes (red and green lines), The incident beam(white arrow), metal balls(white dots) and the diffracted angles θ and θ'.

B Bragg Angle Calculation

Rearranging Eq. 1 and following the discussion above, we obtain two sets of angles at which intensity peaks are expected due to Bragg diffraction:

$$\theta_{\text{Bragg}} = \begin{cases} \sin^{-1}\left(\dfrac{n\lambda}{2d}\right), \\ \sin^{-1}\left(\dfrac{n\lambda}{2\sqrt{2}d}\right) - 45^\circ \end{cases} \tag{3}$$

The arguments of the inverse sine function must lie within the range $[-1, 1]$, which imposes a constraint on the allowed values of n. As a result, only a finite set of Bragg angles is possible. Furthermore, the second expression for θ_{Bragg} can yield negative values. However, since the experimental setup only allows for measurements in the range 0° to 65°, any negative angles are physically irrelevant and should be omitted from consideration.

II Methods

A Experimental Setup

The experimental setup consists of the following components:

- A microwave transmitter (wavelength: 2.4 ± 0.1 cm)
- A receiver
- An analyzer
- A square lattice composed of metal spheres placed 4 cm from one another

Both the transmitter and the receiver operate with a specific polarization, determined by their physical orientation.

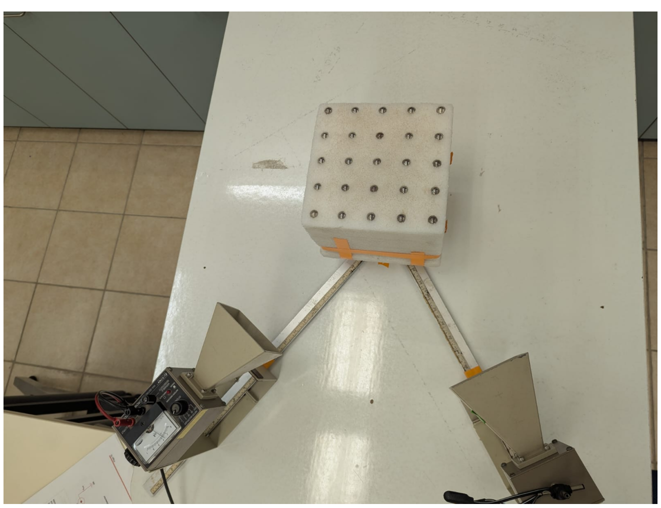

Figure 2: Image of the setup: on the right is the transmitting antenna and the the receiving on on left. In the middle is the square lattice of metal balls

B Uncertainties

- **Emitted Intensity** — The wave's intensity is not constant, but fluctuates around a mean value. This uncertainty is quantified as the standard deviation of each measurement.

- **Angle** — All components were placed manually, which introduces angular imprecision. This uncertainty is estimated as half the smallest division on the calibration scale, i.e., 0.5°.

C Expected Bragg Angles

Using the measured wavelength of the microwave source ($\lambda = 2.86$ cm) and the known lattice spacing ($d = 4$ cm), we used Eq. 3 to calculate the angles at which Bragg diffraction is expected. For the axis-aligned planes, the first and second-order peaks are:

$$\theta_1 \approx 20.9^\circ, \quad \theta_2 \approx 45.6^\circ$$

For the diagonal plane, only the third-order solution falls within the accessible measurement range:

$$\theta_3 \approx 4.3^\circ$$

All other diagonal values yield negative angles and are therefore excluded.

III Results

Figure 3 presents the measured intensity as a function of incident angle. Three local maxima are clearly visible at $4^\circ \pm 0.5^\circ$, $21^\circ \pm 0.5^\circ$, and $47^\circ \pm 0.5^\circ$. The first two peaks align with the calculated Bragg angles: θ_3, θ_1. The third peak deviates from θ_3 by 1.5° which is three standard deviations. This deviation from the theoretical value could be due to the greater influence of unstable emitted intensity at lower values.

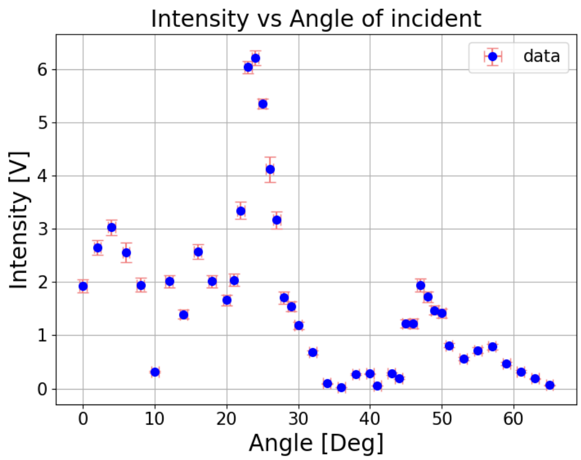

Figure 3: Measured intensity as a function of angle. Blue dots represent the data; red bars indicate measurement uncertainties.

IV Conclusion

In this experiment, we demonstrated that Bragg diffraction can be observed using macroscopic components by replicating a crystal lattice with a Styrofoam cube containing a regular array of metal spheres. Using microwaves with a wavelength of 2.86 cm, we detected clear intensity peaks corresponding to the first and second diffraction orders predicted by Bragg's Law. The measured peak angles closely matched the theoretical values calculated from the known lattice spacing. In addition, we verified that both the transmitter and receiver act as polarizers by confirming a $\cos^2\theta$ dependence in a separate Malus' Law measurement. This step was necessary to validate the use of polarized wave behavior in the diffraction analysis. The agreement between theory and measurement suggests that a scaled-up model may be a useful tool for visualizing and exploring the principles of X-ray crystallography, and indicates that wave interference theory could be applicable across different length scales.

Appendix A – Verification of Polarization via Malus' Law

To confirm that the microwave transmitter and receiver function as polarizers, we measured the transmitted intensity as a function of the angle between their orientations. The resulting data is shown in Figure 4. We fit the data to the form of Malus' Law:

$$I(\theta) = A\cos^2(\theta) + B$$

The fit yielded:

$$A = 2.105 \pm 0.001, \quad B = -0.0529 \pm 0.0007$$

with a clear cosine-squared dependence. The close agreement between the data and the theoretical model confirms that both the transmitter and receiver exhibit polarization behavior, which is essential for analyzing polarized wave diffraction in the main experiment.

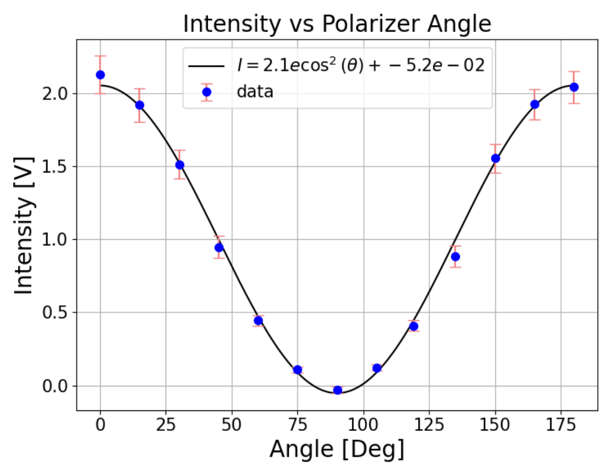

Figure 4: Measured intensity as a function of the angle between transmitter and receiver. The fit follows Malus' Law.